Rectangular Hole Flanging Forming Process Analysis with Finite Element Method

Shasha Dou, Jiansheng Xia

College of Mechanical Engineering, Yancheng Institute of Technology, Yancheng 224051, Jiangsu, China

Abstract
Finite element method is an effective method to analysis the sheet forming process. Using elasto-plastic finite model, Prandtl-Reuss flow rule, Hill48's yield criterion respectively, the Updated Lagrangian Formulation (ULF), and the four degenerated shell element. The friction phenomenon of slippage and viscosity at the boundary interface is based on increment of revision Coulomb rule. An extended r_{min} rule is used to formulate the boundary condition. The simulation is carried out to study the Rectangular Hole-Flanging forming Process by different die structure and parameter. Two steps forming is better than the direct forming, and good distribution sterss and thickness. The results are provided reference for designers and analysts.
Key words: FINITE ELEMENT, SHEET METAL, FORMING PROCESS

1. Introduction

There are the large displacement, large rotation and large strain in metal forming process, which caused by the die shape effect. The punch resistance and side resistance is too large, sone rupture phenomenons of fracture, thinning, wrinkling usually happen. Multi-forming method need to analysis the deep forming products. It reduces the shrinkage of the flange through multi forming, not exceed the bearing force, avoid rupture of sheet forming [1-3].

In the late 1960s, the finite element analysis method was applied in the field of metal forming. According to Von Mises yield criterion, Prandtl-Reuss equations, Love. A. E. H. [4] application shell theory, ignoring the effect of bending, proposed to Speherical, ellipsoid, cylindrical, conical shape, analysed stress and strain distribution. M. Merklein [5] proposed two methods direct reforming and reverse reforming, pointed out the product quality is relationship with the stretch ratio and the lower mould radius.

Farshid Dehghani [6] applicated Barlat-Lian Simulating law and yield large deformation elastoplastic finite element method to analyse the deep forming forming, found earring is an inevitable phenomenon during the forming forming process. Sousa [7] optimized design parameters of V and U bending with the finite element method and Genetic algorithm (GA), those parameters including: punch and die radius, punch displacement and plate force.

2. Methodology

2.1. Virtual work principle

It descripts the elastic-plastic deformation with the updated Lagrangian formulation ULF [6], the Virtual work principle formulation can be shown as follows:

$$\int_{V^E}\left(\ddot{\sigma}_{ij}-e\sigma_{ik}\dot{\varepsilon}_{kj}\right)\delta\dot{\varepsilon}_{ij}dV+\int_{V^E}\sigma_{jk}L_{ik}\delta L_{ij}dV=\int_{S_f}\dot{f}\delta v_i dS \quad (1)$$

where, $\ddot{\sigma}_{ij}$ is the Cauchy stress tensor, $\dot{\varepsilon}_{kj}$ is the rate of stress tensor, $\dot{\varepsilon}_{ij}$ is the strain tensor, σ_{jk} is the rate of strain tensor, $\delta\dot{\varepsilon}_{ij}$ is the virtual strain tensor of the point, δL_{ij} is the virtual velocity gradient tensor of the point, δv_i is the velocity component, $\dot{f}$ is surface force component.

2.2. Constitutive Equations

The element analysis constitutive relation can be written as the formula (2) and (3) follow [8-11].

$$\dot{\sigma} = C^{ep}_{ijmn}\dot{\varepsilon}_{mn} \tag{2}$$

$$C^{ep}_{ijmn} = C^{e}_{ijmn} - \frac{C^{e}_{ijkl}C^{e}_{uv}\frac{\partial f}{\partial \sigma_{kl}}\frac{\partial f}{\partial \sigma_{uv}}}{C^{e}_{kluv}\frac{\partial f}{\partial \sigma_{kl}}\frac{\partial f}{\partial \sigma_{uv}} + H'\frac{\sigma_{uv}\frac{\partial f}{\partial \sigma_{uv}}}{\bar{\sigma}}} \tag{3}$$

Where, $\dot{\sigma}_{ij}$ is Jaumann differential of σ_{ij}, C^{ep}_{ijmn} is the elastic-plastic module, C^{e}_{ijmn} is Elastic module, f is the initial yield function, H' is the strain hardening rate, $\bar{\sigma}$ is Von Mises yield function. the Matrix C^{ep}_{ijmn} can be expressed as the formula (4)(5)(6)(7).

$$\left[C^{ep}\right] = \left[C^{e}\right] - \frac{1}{S}\begin{bmatrix} S_1^2 & S_1S_2 & S_1S_3 & S_1S_4 & S_1S_5 & S_1S_6 \\ & S_2^2 & S_2S_3 & S_2S_4 & S_2S_5 & S_2S_6 \\ & & S_3^2 & S_3S_4 & S_3S_5 & S_3S_6 \\ & & & S_4^2 & S_4S_5 & S_4S_6 \\ & & & & S_5^2 & S_5S_6 \\ & & & & & S_6^2 \end{bmatrix} \tag{4}$$

$$S = -\bar{\sigma}\ H' + S_1\sigma'_{xx} + S_2\sigma'_{yy} + S_3\sigma'_{zz} + 2S_4\sigma'_{yz} + 2S_5\sigma'_{zx} + 2S_6\sigma'_{xy} \tag{5}$$

$$S_1 = 2G\sigma'_{xx},\ S_2 = 2G\sigma'_{yy},\ S_3 = 2G\sigma'_{zz} \tag{6}$$

$$S_5 = 2G\sigma'_{zx},\ S_5 = 2G\sigma'_{zx},\ S_6 = 2G\sigma'_{xy} \tag{7}$$

σ'_{ij} is deviator of σ_{ij}, G is the friction flow potential, $G = \sigma_1^2 + \sigma_2^2$, $\left[C^{e}\right]$ is the formula in minimum strain, which can be expressed as the formula(8) follow[12-13]:

$$\left[C^{e}\right] = \frac{E}{1+v}\begin{bmatrix} \frac{1-v}{1-2v} & \frac{1-v}{1-2v} & \frac{1-v}{1-2v} & 0 & 0 & 0 \\ & \frac{1-v}{1-2v} & \frac{1-v}{1-2v} & 0 & 0 & 0 \\ & & \frac{1-v}{1-2v} & 0 & 0 & 0 \\ & & & \frac{1}{2} & 0 & 0 \\ & & & & \frac{1}{2} & 0 \\ symm & & & & & \frac{1}{2} \end{bmatrix} \tag{8}$$

E is modulus of elasticity, v is Poisson's ratio.

2.3. Finite element formula

Finite element analysis: the structure is divided into many small units which called discrete entity. Based on Large deformation stress and stress rate relation, the finite deformation of update Lagrangian formulation, material constitution relationship, the velocity distribution of each unit is shown as the formula (9)(10)(11):

$$\{v\} = \leq [N]\{\dot{d}\} \tag{9}$$

$$\{\varepsilon\} = \leq [B]\{\dot{d}\} \tag{10}$$

$$\{L\} = \leq [M]\{\dot{d}\} \tag{11}$$

Where, $\{v\}$ is velocity, $\{\varepsilon\}$ is strain rate, $\{\dot{d}\}$ is velocity gradient, $[N]$ is shape function, $\{\dot{d}\}$ is nodal velocity, $[B]$ is strain rate-velocity matrix, $[M]$ is velocity gradient-velocity matrix.

2.4. Friction Processing

There is friction in sheet forming process, so we need to pay attention to materials and tools of the interface conditions. When the material moves along the tool surface curve of the slide, the contact force can be expressed as the formula (12).

$$F = F_l l + F_n n \tag{12}$$

F_l is radial force and F_n is normal force.

2.5. $R_{\min}$ Method

Using the elastic plastic finite element method with large deformation method, also called the Yamada $r_{\min}$ method.

$$r_{\min} = MIN\left(r_1, r_2, r_3, r_4, r_5\right) \tag{13}$$

Where, r_1 is The maximum allowable strain increment, r_2 is the maximum allowable rotation increment, r_3 is the minimum value in all elastic elements, r_4 is contact position between free node and tooling, r_5 is discontent position between free node and tooling.

2.6. Numerical Analysis Flow

The 3d model design with the NX software, which is meshed with NASTRAN software follow. The whole analysis process is as shown in Figure 1.

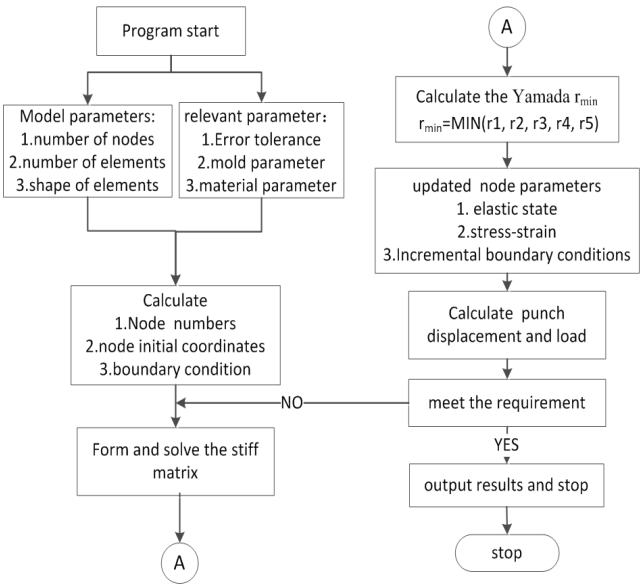

Figure 1. Simulation flow chart

The model structures are composed of punch, die and blank holder, and as shown in Figure 2.

There are two coordinates to solve the problem,

one is the fixed coordinates (X, Y, Z), the other is the local coordinates (ξ, η, ζ). With the right-hand rule, the local coordinates (ξ, η, ζ) is used when nodes contact with the tool, and the fixed coordinates (X, Y, Z) is used when the nodes do not contact with the tool.

The 1/4 model is taken to finite element analysis. The quadrilateral segmentation of degenerated shell element is used in sheet metal meshing, when four point quadrilateral degenerated shell element is used in the die meshing.

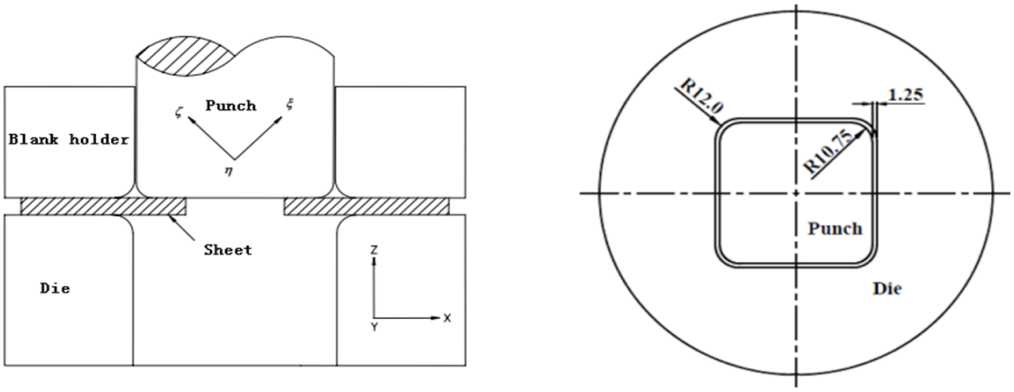

Figure 2. The sheet metal and die size chart

The shape of hole is square, and the edge is round. The length of hole is 62mm, the fillet radius of the hole is 4mm, and the length of edge is 150mm, the radius of the edge is 45mm.

JIS SPCC material stainless steels were provided by a china steel Crop, of which the mechanical properties as shown in Table 1 [12].

Table 1. Mechanical properties of JIS SPCC

Stress-strain relationship: $\bar{\sigma} = 563.64\left(0.011+\bar{\tau}_p\right)^{0.2781}$	
Initial thickness: $t = 0.6mm$	Poisson's ratio: $\upsilon = 0.3$
Yield stress: $\sigma_y = 163.5MPa$	Anisotropy value: r_0=1.71, r_{45} =1.52, r_{90}=2.11
Yang coefficient: E=2.1×10^5 MPa	

3. Results and Discussion

Design three groups of experiments, one step drawing, two step forming and direct forming. Different results were obtained from the simulation results.

3.1. Load and displacement of the punch

The relationship between stroke and forming punch load when square hole flange was shaped by direct forming and two steps forming. As can be seen from the Figure 3, the punch load of two steps forming is lower to direct forming. The reason is there were two types different sizes dies to draw from the two steps drawing process.

After the first forming, the contact area between the sheet and punch is relatively reduced, the punch load decreases with stroke.

So the two steps forming process can improve the formability of sheet.

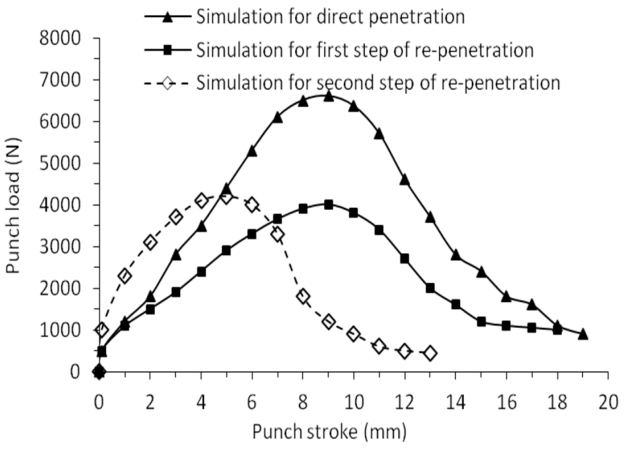

Figure 3. Punch load and stroke diagram

3.2. Stress Distribution Analysis

The main stress will increase with the increasing of relative displacement of the punch in the forming process. It is shown in figure 4.

As shown in Table 2 and figure 5, the stress mainly

concentrates in fillet of die and punch, because of the great Circumferential tensile force, the top value is 496.43Mpa in first step forming, 580.10Mpa in second step forming. The circumferential tensile force is not significant obvious in parallel edge contact area of sheet and punch, so the stress is smaller. By holding the pressure effect, the minimum principal stress in pressure plate clamp area.

Comparison of direct forming and two steps forming processes, the stress is distributed uniformly in the corner of two steps forming. The deformation is smaller than the direct forming in the area of parallel edge contact.

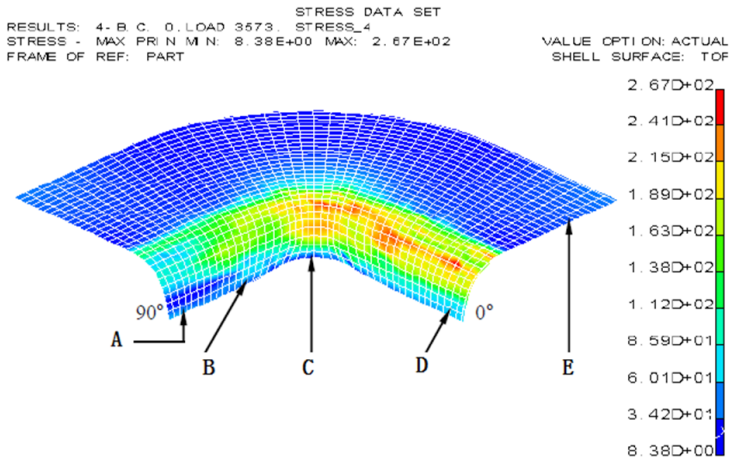

Figure 4. Maximum principal stress distribution

Table 2. The stress distribution

Position	A(Mpa)	B(Mpa)	C(Mpa)	D(Mpa)	E(Mpa)
First-step forming	62.60	39.51	23.67	67.48	36.59
Second-step forming	154.43	146.26	580.10	141.40	28.95
Direct forming	241.23	251.21	592.12	201.65	28.87

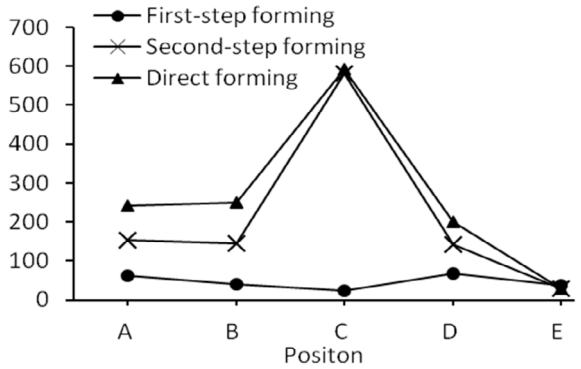

Figure 5. Stress distribution

3.3. Thickness Analysis

After forming, there were different stress in Forming process of the sheet mental. Thickness would be thinner. In order to study the change rules between the thickness and different forming types, two simulation experiments were arranged. One is one stage forming, the other is two stages forming. The position values were measured and recorded as shown in Table 3.

Thickness distribution of sheet can be divided into four regions. The relative positions are from the 0mm to 22mm; the sheet contacts to the punch closely; the thickness is no obvious change.

The second area is from the 22mm to 40mm, the sheet is under the axial stress in the area of die fillet, and thin gradually. The third area is from the 40mm to 52mm, the sheet is squeezed into die accompany with punch movement; the sheet flow is hindered, and the thickness increases, the fourth area is form 52mm to74mm, the thickness change small.

Table 3. The thickness in different relative position and different parameters

Position	first step Square length(mm)			second step Square length(mm)			direct forming Square length(mm)		
	62	61	60	60	59	58	62	61	60
A	0.78	0.78	0.77	0.78	0.78	0.77	0.78	0.77	0.75
B	0.67	0.67	0.66	0.66	0.66	0.66	0.66	0.66	0.64
C	0.49	0.48	0.46	0.49	0.48	0.48	0.44	0.38	0.33
D	0.69	0.68	0.68	0.68	0.68	0.67	0.68	0.68	0.68
E	0.78	0.79	0.78	0.78	0.79	0.78	0.78	0.78	0.77

As shown in figure 6(a), in the first step forming, the sheet slides into die fillet by the influence of the friction, the material flow changes, occurred the thinning phenomenon, the thinnest point location is C, the value is 0.43mm, which is close to rupture (0.62mm).

As shown in figure 6(b), in the second steps forming, the average thickness about the same with the increasing of the punch stroke, and the minimum value C is 0.48mm, which is large than the rupture value, so the forming performance improve.

As shown in figure 6(a), in the direct forming , the average thickness about the same with the increasing of the punch stroke, and the minimum value C is 0.33mm, which is small than the rupture value, so there is a failure of the product.

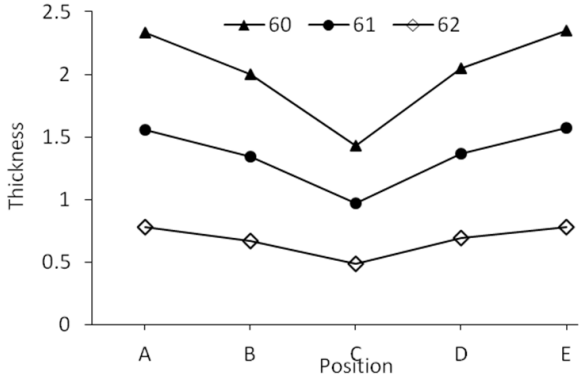

(a) First step forming

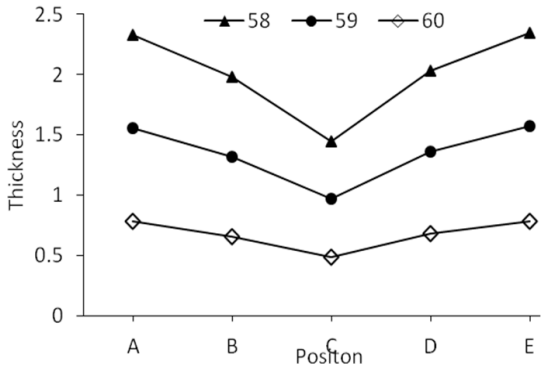

(b) Second steps forming

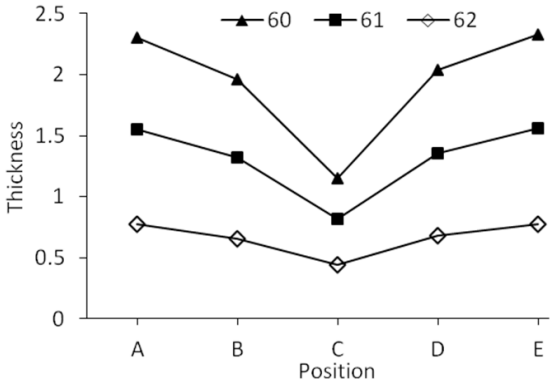

(c) Direct forming

Figure 6. Thickness distribution

3.4. Forming limit analysis

In order to find out the limit thickness of elliptical flange, some experiments are carried out with the different length of sheet, and set the value 0.41mm as the criterion of rupture. As shown in Table 4, if the thickness is thinner, the program will judge that the sheet is in the limit thickness. FR (Forming ratio) LFR (Limit Forming Ratio), and EFR (Excessive Forming Ratio) are referred by Huang and Chen [9] .

FR and LFR values were calculated after the simulation and calculation with different dimension parameter, which was shown inTable4. The conclusion is that LFR value of the second forming is larger than the first forming.

Table 4. The FR and LFR in different dimension parameters

	First step forming R=7.0mm			Second step forming R=7.0mm		
Square length	60mm	61mm	62 mm	60 mm	61 mm	62 mm
FR	1.28	1.26	1.24	1.33	1.28	1.30
LFR	1.26			1.30		

4. Conclusions

(1) During forming process, the stress and the thickness distribution of the figure in the experiment, the experimental value is quite close to the theoretical

value.

(2) In one step forming, the load is greater with the size of the sheet by the relationship between the punch and the load displacement, but the second step reforming, the Maximum stress position is in the corner of the punch, and decreases with the increase of the fillet radius.

(3) Seen from the thickness distribution diagram, the thinnest position is in the corner of the punch and the material was extruded thickly in the end edge of piece. The second step reforming is more good distribution than direct forming.

(4) Under the comparison between direct forming and two steps forming in the analysis of forming limit of square hole-flanging process, the forming limit ratio of sheet is improved from 1.26 to 1.30.

Acknowledgements

This project is supported by National Natural Science Foundation of China (Grant No. 51505408). Jiangsu Ecological building materials and environmental protection equipment Collaborative Innovation Center common technology projects (No. GX2015204). The National Spark Program Project, China (No. 2014GA690214). Jiangsu Intelligent Mould Manufacturing Engineering Technology Research Center.

References

1. Jiansheng Xia, Shasha Dou (2013) Experimental Research on the Flanging Height Adjustment Based on Environmental Way International. *Journal of Applied Environmental Sciences*, 8(20), p.p. 2470-2489.
2. Jiansheng Xia, Shasha Dou (2014)The study on steel elliptical cup forming based on finite element analysis. *Computer Modelling and New Technologies*, 18(10), p.p. 7-13.
3. Jiansheng Xia, Shasha Dou (2014)Numerical analysis of sheet metal U-Bending process. *Computer Modelling and New Technologies*, 18(11), p.p.159-165.
4. Love. A. E. H. A.(2013) *Ttreatise on the Mathematical Theory of Elasticity*. Cambridge University Press: New York.
5. M. Merkleina, J.M. Allwoodb, et al. (2012)Bulk Forming of Sheet Metal. *CIRP Annals - Manufacturing Technology*, 61(2), p.p. 725-745.
6. Farshid Dehghani, Mahmoud Salimi (2015)Analytical and Experimental Analysis of The Formability of Copper-stainless-steel 304L Clad Metal Sheets in Deep Forming. *International Journal of Advanced Manufacturing Technology*, 32, p.p.511-518.
7. L. C. Sousa, C. F. Castro and C. A. C. Antonio. (2006)Optimal Design of V and U Bending Processes Using Genetic Algorithms. *Journal of Material Processing Technology*,172, p.p.35-41.
8. S. Sezek, V. Savaz, B. Aksakal (2010)Effect of die radius on blank holder force and forming ratio: a model and experimental investigation. *Mater. Manuf. Process*, 25(7), p.p.557-564.
9. Y. M. Huang and K. H. Chien (2002) Influence of Cone Semi-Angle on the Formability Limitation of the Hole-Flanging Process. *International Journal of Advanced Manufacturing Technology*, 19(8), 597-606.
10. V. Vafaeesefat (2011)Finite element simulation for blank shape optimization in sheet metal forming. *Mater. Manuf. Process*, 26, p.p.93-98.
11. J Xu, Z Tu, N Hu (2015) Rotation Invariant Constitutive Relation for Reynolds Stress Structure Parameter. *Applied Mathematics and Mechanics*, 36(4), p.p. 517-522.
12. H. Laurenta, J. Coëra, b, P.Y. Manacha, M.C. Oliveirab, L.F. Menezesb (2015) Experimental and Numerical Studies on The Warm Deep Forming of An Al-Mg Alloy. *International Journal of Mechanical Sciences*, 93, p.p. 59-72.
13. Shasha Dou (2015) Numerical Analysis of Elliptical Flange Hole Forming Process. *Metallurgical and Mining Industry*, 7(7), p.p. 344-351.